Adhesion of bone cells to ion-implanted titanium

S. NAYAB[1,2], L. SHINAWI[2,3], J. HOBKIRK[3], T. J. TATE[4], I. OLSEN[2]*, F. H. JONES[1,]
[1]*Departments of Biomaterials, Eastman Dental Institute for Oral Health Care Sciences, University College London, 256 Gray's Inn Road, London WC1X 8LD, UK*
E-mail: i.olsen@eastman.ucl.ac.uk
[2]*Periodontology*
[3]*Prosthetic Dentistry*
[4]*Department of Electrical and Electronic Engineering, Imperial College of Science, Technology and Medicine, Exhibition Road, London SW7 2BT, UK*

The use of ion-implantation to encourage osseointegration has been investigated using an *in vitro* model cell culture system and surface analysis. Polished titanium discs were implanted with calcium, potassium and argon ions. The adhesion of bone-derived cells was measured using radioactively labeled cells and the morphology examined using scanning electron microscopy. Similar numbers of cells were found to adhere to the potassium and argon-implanted titanium as to control (non-implanted) titanium. However, adhesion to the calcium-implanted titanium discs was significantly reduced. Moreover, although the cells were found to be well spread on the calcium and potassium-implanted titanium, a much greater proportion of cells appeared to remain rounded and poorly attached on the argon-implanted surface. These differences are discussed in relation to the observed surface roughness and chemistry, which were assessed using interferometry and X-ray photoelectron spectroscopy, respectively.

Introduction

The value of titanium-based materials for dental and orthopedic implants stems primarily from their advantageous bulk mechanical properties (in particular strength, rigidity and resistance to corrosion [1]) in combination with a high degree of biocompatibility which is largely attributable to their surface properties. Of particular value for load bearing applications is the ability of commercially pure Ti to form an osseointegrated interface with bone [2]. Freshly prepared Ti surfaces react rapidly with oxygen in the surrounding environment, becoming covered in a thin (1–10 nm), dense layer of oxide which is able to withstand physiological environments without disintegration [3]. It is this oxidized surface layer, rather than Ti in the metallic state, that interacts with cells at the implant–tissue interface and thereby plays a major role in modulating the events responsible for tissue regeneration around the implant.

Both surface chemistry and topography affect cellular response [4] and a considerable body of work has been devoted to modifying these properties in order to provide a more effective interface for osseointegration. In the case of Ti, changes in the macro- and microscopic topography of the surface are commonly achieved by machining, sandblasting, sandblasting and acid etching (SLA surfaces) and plasma spraying with Ti (TPS surfaces) [3].

Interest in chemical modification has been stimulated by the successful use of coatings such as hydroxyapatite, which provide an inorganic surface with physicochemical characteristics similar to those of bone [5, 6]. Disadvantages of such coatings, including fracture, weak adhesion leading to delamination and potential problems with bacterial colonization, have led to the search for alternative direct chemical treatments. One approach involves surfaces designed to encourage apatite formation from body fluids, thus creating the bone-like surface chemistry considered to be beneficial for osseointegration. Treatments include H_2O_2 with [7] or without [8] chloride ions, alkali solutions, with or without heat treatment [9–12], calcium ion containing solutions [13, 14] and etching with HCl and H_2SO_4 [15, 16]. A second strategy has been to attach specific biomolecules to the Ti surface in order to create an organic surface chemistry favorable to interacting target cells. Examples include silanization of the surface, where biological responses may depend on the terminal group [17] or the use of cross-linking molecules to attach biologically active mediators [18]. However, the response of target tissues to differences in surface chemistry is not currently well-understood at the cellular level.

In vitro biological evaluation can provide fundamental information about the events which occur at bone/material interfaces. Cell culture techniques enable

*Author to whom all correspondence should be addressed.

precise measurements to be made of biological parameters such as adhesion, morphology, biosynthetic function, gene activity and cell death [19]. Together with in-depth analyses of chemical and topographical surface properties, such studies can provide essential data about the precise relationship between the characteristic features of a material and its real or potential clinical efficacy.

One technique whereby surface chemistry can be altered under controlled conditions is ion-implantation. In this process, specific ionic species are incorporated directly into the surface by electrostatically accelerating an energetic beam of ions into the substrate. Developed originally in the 1950s, this technique is routinely used in applications such as integrated circuit fabrication [20] due to its speed, homogeneity and high ''dopant'' purity. Shallow layers can be implanted with high doping gradients, allowing near surface modification without affecting the mechanical properties of the bulk material. Furthermore, since the dosage can be precisely controlled, it is a highly valuable method of fabricating controlled and reproducible surface compositions for systematic studies.

Several investigations have utilized ion-implantation to alter the surface chemistry of Ti, the most biologically promising of these being the implantation of calcium ions. Hanawa *et al*. [21, 22] demonstrated *in vivo* that the implantation of Ca^+ ions into Ti surfaces enhanced osseointegration and the formation of new osteoid tissue. However, other studies of Ca- and P-ion-implantation into Ti found no beneficial effect on cell viability or alkaline phosphatase (ALP) activity, despite increased corrosion resistance [23]. Such contradictory findings, as underlined by Howlett [24], highlight the importance of further studies of the effects of ion-implantation on biocompatibility and the need to clarify the underlying mechanisms responsible for beneficial or adverse cellular responses.

The present study was therefore undertaken to examine the effects of modification of Ti surfaces by implantation of calcium, potassium and argon on the response of bone cells *in vitro*. Ca was selected because it has a number of essential biological functions and has previously been documented in the literature, while K and Ar were chosen because their atomic masses are similar to that of Ca and they are therefore expected to implant in a similar manner. This is important because beam damage to the substrate may also affect the surface chemistry, as demonstrated by the observation of enhanced HeLa cell attachment on polystyrene after implantation of chemically inert ions [25]. Although the chemistries of the selected ions differ, they should have a similar physical effect on the Ti lattice during implantation, thereby allowing chemical and physical effects to be separated.

Materials and methods

Preparation of ion-implanted Ti discs

Commercially pure Ti discs (grade 1; 1 mm thick and either 8 or 14 mm diameter as noted) were polished on one face to a mirror finish using 1200–2400 silicon carbide grit followed by chemical cloth with a colloidal silica suspension in 5% H_2O_2. They were then cleaned by ultrasonication in acetone followed by deionized water. Ion-implantation was carried out using a Whickam 200 keV implanter, at an implantation energy of 40 keV. The 14 mm diameter discs were implanted with $^{40}Ca^+ (1 \times 10^{17}\,cm^{-2})$, $^{39}K^+ (1 \times 10^{17}\,cm^{-2})$ and $^{40}Ar^+ (2 \times 10^{17}\,cm^{-2})$ ions and were subsequently used for cell culture work and surface chemical analysis. Surface roughness was assessed using the 8 mm diameter discs implanted with $Ca(1 \times 10^{17}\,cm^{-2})$, $K(1 \times 10^{17}\,cm^{-2})$ and $Ar(1 \times 10^{17}\,cm^{-2})$ ions.

Cell culture

Both the control (non-implanted) and ion-implanted Ti discs were sterilized by ultraviolet light prior to cell culture and stored at room temperature in a desiccator. The MG63 cell line, derived from an osteogenic sarcoma of a 14-year-old male [26], was cultured in Dulbecco's modified Eagle's medium (DMEM) supplemented with 10% fetal calf serum (FCS), 100 IU ml^{-1} penicillin, 100 μg ml^{-1} streptomycin and 2 mM *L*-glutamine and incubated at 37 °C in a humidified atmosphere of 5% CO_2 in air.

Cell adhesion – quantitative

To measure cell adhesion, actively dividing cultures of MG63 cells culture were ''tagged'' by radiolabeling for 18 h with [^{3}H] thymidine (44 Ci $mmol^{-1}$), a radioactive precursor of DNA, at a concentration of 1 μCi ml^{-1}. The radiolabeled cells were harvested, washed and a small aliquot removed for determination of radioactivity and for measuring cell number using a hemocytometer. The cells were then seeded in duplicate onto control non-implanted Ti and Ca-implanted Ti, K-implanted Ti and Ar-implanted Ti discs in 24-well plates, at a density of 2×10^4 cells in 0.5 ml of DMEM (14 mm diameter) or 2×10^3 cells in 0.05 ml of DMEM (8 mm diameter). These were incubated for 4 h at 37 °C, after which the non-attached cells were removed by aspiration and the attached cells washed twice with phosphate-buffered saline (PBS). 0.5 ml of 10% ice-cold trichloroacetic acid (TCA) was added for 10 min to precipitate the DNA and the discs were then washed twice with cold 10% TCA. The DNA was dissolved in 0.25 ml of 1% sodium dodecyl sulfate (SDS) and transferred to scintillation vials. Radioactivity remaining associated with the discs was determined by liquid scintillation spectroscopy (WALLAC 1409 liquid scintillation counter) and used as a measure of the number of attached cells. This was calculated from the specific activity of the original cell suspension (dpm/10^6 cells).

Cell adhesion – qualitative

To determine whether the morphology of the cells was affected as a result of ion-implantation, the cultures were examined by scanning electron microscopy (SEM). 2×10^4 MG63 cells were seeded onto control and ion-implanted discs in 1 ml of complete medium per well. Cells were allowed to adhere to the substrates by incubating at 37 °C for 4 h. The discs were then removed,

transferred to fresh dishes, washed with PBS and fixed overnight with 3% glutaraldehyde in 0.1 M cacodylic acid buffer. They were then sequentially dehydrated in alcohol (20%, 50%, 70%, 90% and 100%) for 10 min each, immersed in hexamethyl disilazane solution, a critical point drying fluid, for 1.5 min and then air-dried for 1 h at room temperature. A thin layer of gold/palladium was sputter coated onto the discs using a Polaron E5000 (Quorum Technologies, UK). The discs were then visualized using a Cambridge 90B SEM (LEO Electron Microscopy Ltd) at an acceleration voltage of 15 kV and photographed. This morphological examination of the cells on Ti surfaces was repeated three times, observing five individual fields for each sample in order to identify representative cell–surface interactions.

Surface analysis

Average RMS roughness ($R_q/\mu m$) was the most widely explored topographical parameter. A white light scanning interferometer (Zygo, New View 200) was used to measure the average RMS roughness (from a minimum of three separate areas) for each of six samples of the as-polished and as-implanted titanium. The values for the six separate samples were then used to find the average values and standard deviations given in the results.

Surface chemistry was analyzed by X-ray photoelectron spectroscopy, using the Scienta ESCA300 spectrometer at the RUSTI facility at Daresbury Laboratory. The spectrometer (base pressure $< 2 \times 10^{-9}$ mbar) is equipped with a rotating anode Al K_α ($h\nu = 1486.6$ eV) X-ray source with a-seven crystal, double focusing monochromator and a 300-mm radius hemispherical analyzer with multi-channel detector. The overall instrument resolution is a minimum of 0.30 eV. Spectra were collected in constant analyzer energy (CAE) mode at a pass energy of 150 eV. Samples were not prepared in any way after placing in the UHV chamber. Spectra were recorded at normal emission and are shown normalized to the $Ti2p_{3/2}$ peak height. Binding energy alignment was carried out so that the Ti2p peak maximum of the native Ti sample was aligned at 458.8 eV as previously discussed [27], assuming that spectra from all the samples were aligned at their Fermi energies. Quantification was carried out by measuring peak areas after linear background subtraction and correcting for atomic sensitivity factors according to Wagner *et al*. [28]. No allowance was made for the variation in the transmission function of the instrument with kinetic energy.

Implantation simulation

Ion-implantation is an energetic process in which the host lattice is disturbed by the incident ions. The degree of disturbance can be estimated by a parameter known as the displacements per atom, or dpa, which may be interpreted as the number of times that any lattice atom is involved in a collision in which the energy is greater than the lattice energy. X ray diffraction usually indicates that samples are amorphous if the dpa exceeds 0.1, that is, if one atom in every 10 has been displaced. The Monte Carlo implantation simulation code, SRIM [29], was used to estimate dpa for the high dose implant regimes used. A second simulation program, Profile code [30], was used to predict the ion range and implantation profile in the Ti target.

Statistical analysis

Experiments were conducted three times and significant differences of MG63 cell adhesion between control and ion-implanted Ti were established using the Student's *t* test for paired samples. Statistical significance levels were determined at p values of ≤ 0.05.

Results

Cell adhesion – quantitative

The adhesion of the bone cells to the Ti discs was measured *in vitro* as described above. In three separate experiments it was found that 62%, 57% and 43% (average 54%) of the cells which were added initially had attached to the control non-implanted Ti discs during a period of 4 h. The results in Fig. 1 show that, under the same conditions, adhesion of the MG63 cells to the K- and Ar-implanted Ti discs was the same as to the non-implanted Ti (95.0% and 90.4% of that of the control, respectively). In contrast, the adhesion of the cells to the Ca-implanted Ti discs was significantly reduced, to an average of 69.4% compared with control levels ($p = 0.01$).

3.2. Cell adhesion – qualitative

Examination of cell adhesion by SEM revealed that MG63 cells seeded onto the Ca–Ti and K–Ti discs appeared to be more highly spread, with an increased cell to substrate contact ratio, than those seeded on the non-implanted control Ti discs (Fig. 2). Cells on the Ar–Ti discs were also highly flattened and well spread, but on this particular substrate it was apparent that there was a higher proportion of cells which had attached but not yet spread, as shown in Fig. 2.

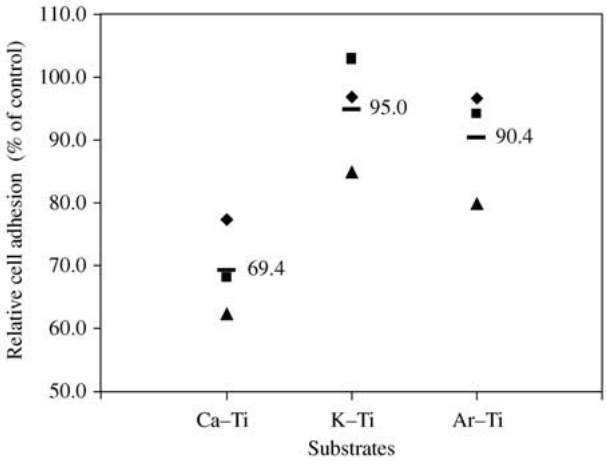

Figure 1 Adhesion of MG63 cells to Ca–Ti, K–Ti and Ar–Ti compared with control non-implanted discs. The radioactivity remaining on the implanted and control Ti discs was measured in three separate experiments. The results of each experiment and the means (numbers and horizontal lines) are shown relative to binding to the control Ti, defined as 100%.

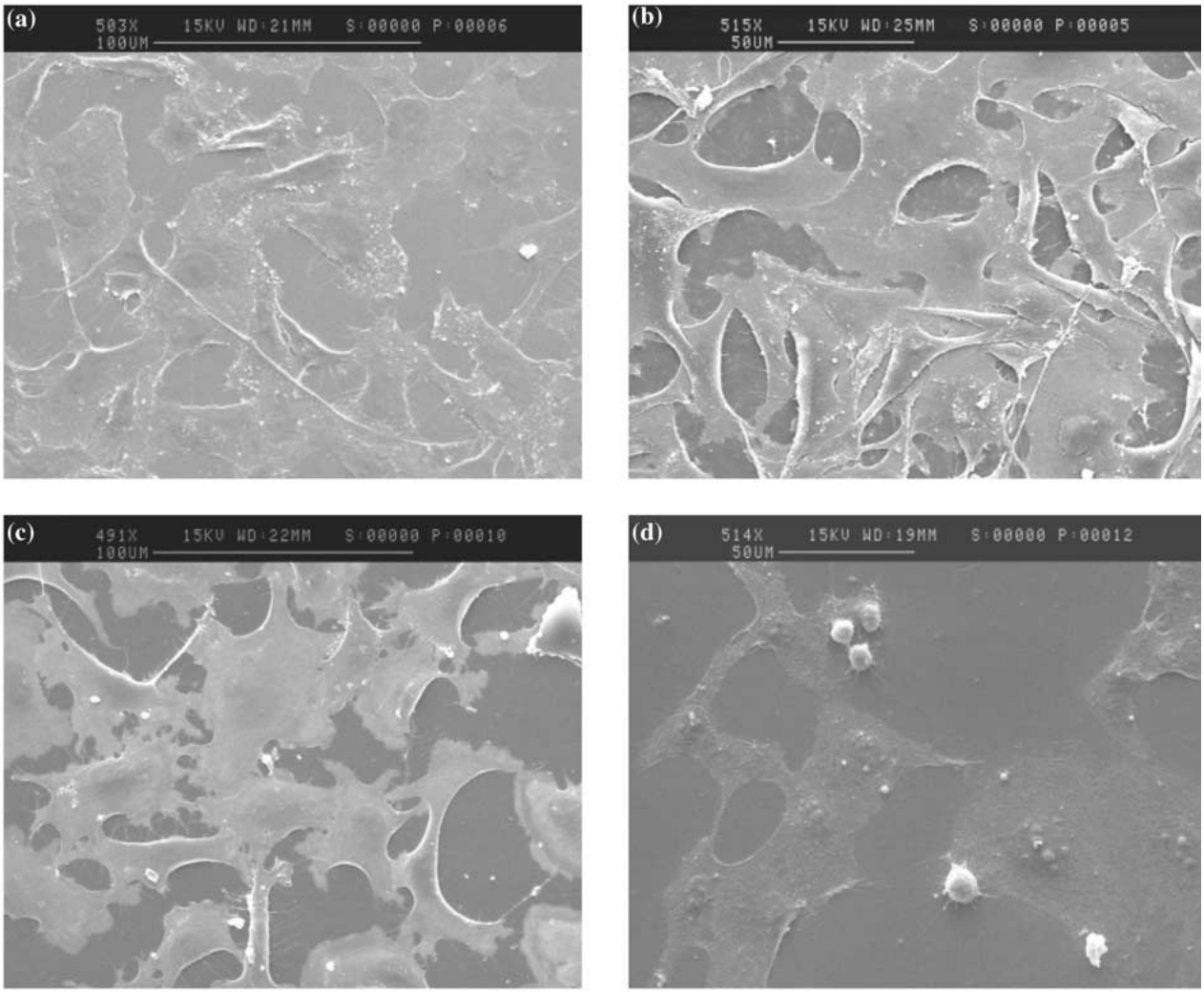

Figure 2 SEM micrographs of MG63 cells attached to (a) Ti, (b) Ca–Ti, (c) K–Ti and (d) Ar–Ti discs after 4 h of incubation. Note the relatively fewer number of attached cells in (b) and the higher proportion of rounded cells in (d). Magnification 491–500×, as indicated.

Surface analysis

The RMS average roughness ($R_q/\mu m$) of the samples is shown in Table I. No significant difference in roughness was observed between the implanted and non-implanted samples. It is therefore unlikely that the higher dose Ar-ion implanted samples, as used for the cell culture studies, would have a significantly greater roughness although this was not actually measured due to unavailability of high-dose samples at the time of roughness measurement.

TABLE I Effect of ion-implantation on surface roughness of Ti

Sample	Implantation dose (ions cm^{-2})	Average RMS roughness/(μm)
Ti	—	0.054 ± 0.021
Ca	1×10^{17}	0.071 ± 0.009
K	1×10^{17}	0.082 ± 0.013
Ar	1×10^{17}	0.075 ± 0.027

Widescan XPS spectra (not shown) displayed all the expected peaks. For non-implanted Ti, the main peaks observed were Ti2p, O1s and C1s. For the implanted samples, these were accompanied by peaks due to the implanted ions. The strongest peaks were the Ca2p (346.0 eV), K2p (293.0 eV) and Ar2p (242.3 eV) peaks for Ca–Ti, K–Ti and Ar–Ti, respectively. Narrow scans of the most important regions of the spectra are shown in Fig. 3. Surface concentrations of these elements, estimated from measured peak areas, are given in Table II as elemental ratios relative to Ti.

The implanted ion peaks are shown in Fig. 3(a). As expected, each is a simple spin–orbit doublet. The most important point to note is that the Ar2p peaks are considerably weaker than the corresponding Ca2p and K2p peaks, despite the Ar^+ ion-implantation dose being twice that of Ca^+ and K^+. This is emphasized by the estimated elemental ratios; Ar/Ti = 0.04, compared to Ca/Ti = 0.31 and K/Ti = 0.22 for the Ca- and K-implanted samples, respectively.

Fig. 3(b) shows the Ti2p core-level XPS spectra from the samples before and after ion-implantation. As expected, the non-implanted sample (uppermost spectrum) showed major features at 458.8 and 464.5 eV due to the $2p_{3/2}$ and $2p_{1/2}$ spin–orbit doublet from Ti in the +4 oxidation state. These arise due to the presence on the surface of the thin oxide overlayer. The sharp feature at $\sim$ 453.7 eV is the $2p_{3/2}$ component of the spin–orbit doublet from the underlying Ti metal (Ti^0). Between the Ti^0 and Ti^{4+} peaks there is a small amount of intensity indicative of reduced oxide environments. These assignments are in good agreement with previous work on

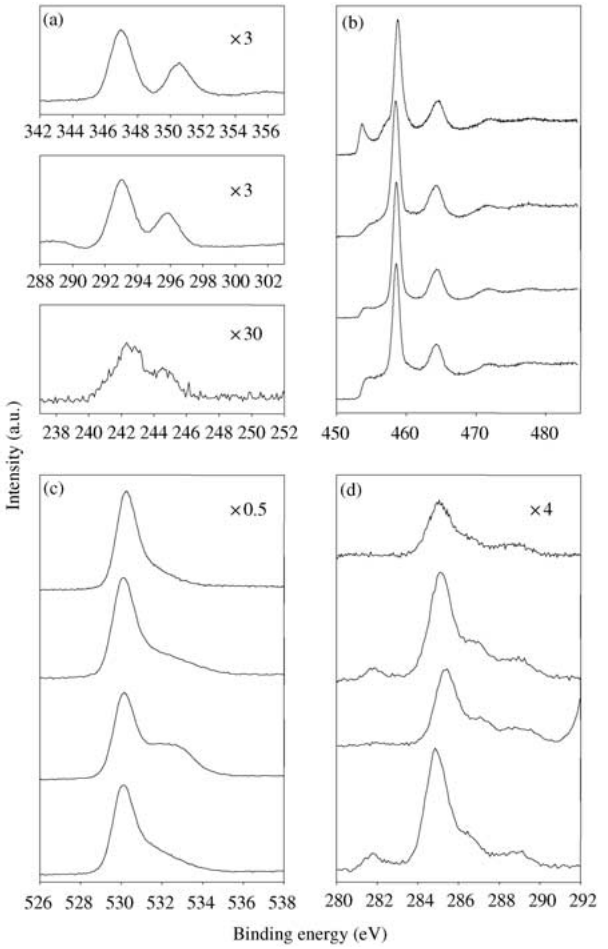

Figure 3 Core level X-ray photoelectron spectra from (top to bottom) non-implanted Ti, Ca–Ti, K–Ti and Ar–Ti: (a) The implanted ion regions, Ca2p, K2p and Ar2p (note the absence of a spectrum from non-implanted Ti); (b) the Ti2p region; (c) the O1s region and (d) the C1s region.

native Ti [31]. From this XPS spectrum it is possible to calculate the approximate thickness of the native oxide layer prior to implantation by comparing the intensities of the Ti peaks from the metal and oxide oxidation states. Although this procedure makes a number of assumptions, including homogeneity of the oxide layer and a well-defined interface with the underlying metal, it is nonetheless possible to estimate an oxide layer thickness of ~ 70 Å.

After implantation, the spectra were still dominated by Ti^{4+} peaks, indicating that the majority of surface Ti remains in the same oxidation state despite the ion-implantation. However, the degree of reduced species (Ti metal and reduced oxides) to low binding energy of the main Ti^{4+} $2p_{3/2}$ peak was observed to vary according to the type of implanted ion. None of the implanted-Ti spectra show the sharp well-defined Ti^0 peak observed for the native metal (Fig. 3(b)). Instead, a broader feature can be seen in each case, which extends from the edge of the Ti^{4+} $2p_{3/2}$ peak down to ~ 453.1 eV. The lack of a clear Ti^0 peak makes it impossible to estimate the thickness of the oxide layers after implantation.

TABLE II Elemental ratios approximated from implantation simulations, compared with those measured using XPS

Ion, X	Dose/10^{17} (ions cm^{-2})	Calculated X/Ti	Measured ratios		
			X/Ti	O/Ti	C/Ti
None	—	—	—	1.73	0.44
Ca	1	0.29	0.22	2.37	1.05
K	1	0.31	0.31	2.70	0.73
Ar	2	0.55	0.04	1.85	0.94

The C1s and O1s peaks are also shown (Fig. 3(c) and (d)). Non-implanted Ti (uppermost spectra) was always found to be contaminated with carbon, as well as having a large O1s peak due to the oxidation of the surface. The C1s peak from the non-implanted Ti (Fig. 3(d)) shows three resolvable components, centered at 285.0, 286.4 and 288.6 eV, which are most probably attributable to hydrocarbon-like carbon, carbon bonded to a single O or N atom and carbon bonded to two N or O atoms. From peak area measurements, the ratio of different types is 60 : 24 : 16. The O1s spectrum (Fig. 3(c)) shows a maximum at 530.3 eV due to oxygen in the -2 (oxide) oxidation state. The peak has a tail to higher binding energies that is indicative of the presence of oxygen bound to the surface both as –OH and H_2O [32].

After ion-implantation, the O1s peak shapes (Fig. 3(c)) remained largely unaltered for the Ca- and Ar-implanted samples. For the K-implanted sample, however, the intensity of the higher binding energy components was considerably increased, suggesting that there was significantly more bound –OH and H_2O on the surface. It is important to note that this was not always observed for K-implanted samples alone; there was often a higher proportion of high binding energy species on all types of surface. In general, however, this was found to be greater on samples implanted with Ca or K.

The C1s spectra recorded from the ion-implanted samples (Fig. 3(d)) indicate an increased amount of carbon on all of the implanted samples. The peak shape remained largely unaltered, aside from the presence to low binding energy (281.7–281.9 eV) of a small feature associated with the presence of carbon in the form of carbide. By peak fitting, the ratios of the three peaks were found to be 60 : 24 : 16 for Ca–Ti, 57 : 28 : 15 for K–Ti and 63 : 25 : 12 for Ar–Ti.

Implantation simulation

SRIM and PROFILE CODE simulations [29, 30] of implantation into amorphous TiO_2 at the beam energy and ion doses used in this study indicated sputtering of 599 Å of material for Ca^+-implantation, 566 Å for K^+-implantation and 1086 Å for Ar^+-implantation (for which the dose was twice that of the other ions). The depths sputtered are all considerably more than the estimated thickness of the native oxide layer on the Ti substrate. Simulations of implantation into Ti were therefore carried out and the concentrations of implanted ions present at the surface were estimated to be $[Ca] = 1.62 \times 10^{22}$ ions cm^{-3}, $[K] = 1.73 \times 10^{22}$ ions cm^{-3} and $[Ar] = 3.13 \times 10^{22}$ ions cm^{-3}. From this, approximate elemental ratios of the ions, X, to Ti (X/Ti) were estimated and are shown in Table II, where they are compared with the values measured using XPS. For Ca–Ti and K–Ti the measured and predicted values are very similar, while for Ar–Ti the measured ratio is around a tenth of the predicted value. In all cases, the dpa

predicted from the SRIM simulations reached a value of 1 or above, over the range from the surface to a depth of 35 nm, at a dose of about 1×10^{15} ions cm^{-2}. Increasing the dose beyond this value will not appreciably alter the amount of radiation damage, so the implanted samples are likely to have similar amounts of damage, despite being implanted at different (high) doses.

Discussion

Both qualitative and quantitative studies indicate that ion-implantation can affect the adhesion of MG63 cells to Ti surfaces. This effect appears to depend on the nature of the implanted ion. Thus, while implantation with Ar and K did not change the number of cells which attached to the surface, cell adhesion appeared to be significantly inhibited by the implantation of Ca ions. The morphological appearance of the attached cells was also found to be related to the type of ion-implanted. Thus, whereas Ca- and K-implanted surfaces resulted in a high degree of cell spreading, at least as extensive as that on the control Ti, implantation of Ar ions resulted in a notably lower degree of cell spreading, with an enhanced proportion of the attached cells remaining rounded on the surface. Although the precise reason for these effects is not known, it is likely to be related to the ion-implantation process itself and the consequent modification of the Ti surface.

During ion-implantation, the transfer of energy to the atoms and ions in the Ti/oxide lattice results in their displacement and/or sputtering out of the surface. This creates a largely amorphous surface and influences the depth profile of the implanted ions. It is clear from the implantation simulations that the oxide layer is fully removed during the implantation process, with subsequent implantation occurring into Ti metal itself. Unlike Ca–Ti and K–Ti, the ratio of implanted ions to Ti for the Ar-implanted sample (Ar/Ti) is very much smaller than the value predicted by the simulation (Table II). It is possible that this inert ion is not trapped in the near surface region during implantation. Instead it may have sufficient energy to escape from the surface or to penetrate deeper into the sample (beyond the XPS sampling depth of ~ 100 Å).

Despite the removal of the oxide layer by sputtering during the ion-implantation process, the Ti2p XPS spectra from the implanted samples indicate that the surfaces primarily contain Ti in the $+4$ oxidation state (Fig. 3). This is likely to be a result of the extreme radiation damage that occurs during ion-implantation. The implanted surfaces will be reactive, leading to rapid oxide re-growth when the samples are removed from the implanter's vacuum environment. The layer formed contains the implanted ions, but may not be fully amorphous. Although it is not possible to estimate the layer thickness, the absence of a Ti^0 peak due to the underlying bulk metal indicates that it is thicker than the sampling depth of XPS (~ 100 Å). The intensity of the low binding energy features due to reduced Ti species ($OS < +4$) is implanted-ion dependent. This may be important, since the presence of Ti^{3+} defect states at the surface of nominally ''perfect'' TiO_2 single crystals can significantly affect surface reactivity [33].

The other major differences between implanted and non-implanted surfaces are the amount of hydroxide/water and the amount and nature of carbon on the surface. Implanted surfaces were generally found to show more C than non-implanted surfaces (Fig. 3(d)) and the C/Ti and O/Ti ratios were always much greater than the ratio of implanted ion (X/Ti), suggesting that these changes in surface chemistry may be as important as the presence of the implanted ions, if not more so.

The presence of hydroxyl groups has been implicated in aiding the nucleation of apatite-like phases on Ti surfaces [9] and might therefore result in a ''conditioned'' surface more prone to cell attachment or spreading. In the current experiments, significantly increased OH levels were most commonly observed on Ca- and K-implanted surfaces. Given the large degree of variation between samples, however, it is likely that the amount of OH observed depends not only on the type of implanted ion, but also the sample preparation, storage atmosphere and duration of storage of the samples. The additional carbon present on the surfaces after ion-implantation may result from contamination during or after the implantation process. The presence of carbide is likely to be due to the transfer of energy from implanting ions to carbon present as contamination on the surface with subsequent embedding and reaction, although a balance with surface sputtering must be maintained.

In summary, the main differences between the implanted and non-implanted surfaces are chemical, since the surface roughnesses measured after implantation were not significantly different from those measured prior to implantation. It is notable, however, that none of the surface characteristics examined are readily correlated with the results of the cell culture studies. The type and amount of carbon present does not appear to be sufficiently different between the samples to account for the observed variation in cell adhesion. Although the increased OH concentration on the Ca- and K-implanted surfaces could be responsible for the high degree of cell spreading, perhaps via an increased rate of calcium phosphate formation as has been observed on surfaces implanted with Ca [34, 35] or Na [36], this does not explain the decreased adhesion on the Ca-implanted surface. The high degree of cell spreading on this surface nevertheless suggests that there has been no deleterious biological effect, despite the presence of fewer cells. Protein binding at the surface may also be at least partially responsible for decreased adhesion to Ca-implanted Ti. For example, treating Ti with $CaCl_2$ to give a Ca^{2+}-rich surface has been shown to create a surface which selectively adsorbs the same proteins from human serum as hydroxyapatite [37], with potentially important consequences for both cell attachment and cell spreading.

The apparently less than optimal spreading on the Ar-implanted surface is of particular interest in view of the inert nature of these implanted ions. Although there is only a low concentration of Ar at the surface, it is possible that the presence of this inert element inhibits the adsorption of one or more species required for the cells to become well spread. A second possibility is that the cellular response is governed in this case by the disruption occurring to the surface during the ion-

implantation process itself. Since the radiation damage is similar for all the surfaces (as evidenced by the very high dpa values), similar effects might be expected for the three implanted surfaces. These were not observed. It is possible that the effect of surface damage may be outweighed by the presence of the ''active'' ions such as in the K–Ti and Ca–Ti surfaces. Another possibility is that the nature of the implanted ion significantly affects the re-growth of the oxide layer. Studies are currently in progress to determine whether the presence of these implanted ion species selectively modulates the functional activity of the cells and thus their potential clinical efficacy.

Conclusion

It has been shown that MG63 cell adhesion to ion-implanted Ti is dependent on the specific ion used for implantation. The observed response may be due to the disruption caused to the Ti surface during the implantation process, as well as to the presence of the implanted ions. The results suggest that certain ions, or combinations of ions, could be used to control the early events in bone cell adhesion to Ti implants.

Acknowledgments

This work was supported by an EPSRC fast stream grant (FHJ) and a BBSRC PhD studentship (SN). Additional funding was provided by the Eastman Foundation for Oral Research and Training (EFFORT). The authors are grateful to D. McPhail (Imperial College of Science, Technology and Medicine, UK) for access to the Zygo interferometer and to D. S. L. Law (RUSTI facility, Daresbury Laboratory) for technical help with the Scienta spectrometer.

References

1. D. BROWN, *Brit. Dent. J.* **182**(10) (1997) 393.
2. T. ALBREKTSSON, P.-I. BRÅNEMARK, H. A. HANSSON and J. LINDSTRÖM, *Acta Orthop. Scand.* **52**(2) (1981) 155.
3. M. TEXTOR, C. SITTIG, V. FRAUCHIGER, S. TOSATTI and D. M. BRUNETTE, in ''Titanium in Medicine'', edited by D. M. Brunette, P. Tengvall, M. Textor and P. T, (Springer-Verlag, Berlin, 2001) p. 172.
4. F. H. JONES, *Surf. Sci. Rep.* **42**(3–5) (2001) 79.
5. K. DE GROOT, J. G. C. WOLKE and J. A. JANSEN, *Proc. Inst. Mech Eng. H* **212**(H2) (1998) 137.
6. J. L. ONG and D. C. N. CHAN, *Crit. Rev. Biomed. Eng.* **28**(5–6) (2000) 667A.
7. J. PAN, H. LIAO, C. LEYGRAF, D. THIERRY and J. LI, *J. Biomed. Mater. Res.* **40**(2) (1998) 244.
8. C. OHTSUKI, H. IIDA, S. HAYAKAWA and A. OSAKA, *ibid.* **35**(1) (1997) 39.
9. H.-M. KIM, F. MIYAJI, T. KOKUBO and T. NAKAMURA, *ibid.* **32**(3) (1996) 409.
10. H.-M. KIM, F. MIYAJI, T. KOKUBO and T. NAKAMURA, *J. Ceram. Soc. Jpn.* **105**(2) (1997) 111.
11. H.-M. KIM, F. MIYAJI, T. KOKUBO and T. NAKAMURA, *J. Mater. Sci.: Mater. Med.* **8**(6) (1997) 341.
12. S. NISHIGUCHI, H. KATO, H. FUJITA, H. M. KIM, F. MIYAJI, T. KOKUBO and T. NAKAMURA, *J. Biomed. Mater. Res.* **48**(5) (1999) 689.
13. T. HANAWA, M. KON, H. UKAI, K. MURAKAMI, Y. MIYAMOTO and K. ASAOKA, *ibid.* **34**(3) (1997) 273.
14. D. G. KIM, M. J. SHIN, K. H. KIM and T. HANAWA, *Biomed. Mater. Eng.* **9**(2) (1999) 89.
15. H. B. WEN, J. G. C. WOLKE, J. R. DE WIJN, Q. LIU, F. Z. CUI and K. DE GROOT, *Biomaterials* **18**(22) (1997) 1471.
16. H. B. WEN, Q. LIU, J. R. DE WIJN, K. DE GROOT and F. Z. CUI, *J. Mater. Sci.: Mater. Med.* **9**(3) (1998) 121.
17. C. N. SUKENIK, N. BALACHANDER, L. A. CULP, K. LEWANDOWSKA and K. MERRITT, *J. Biomed. Mater. Res.* **24**(10) (1990) 1307.
18. A. NANCI, J. D. WUEST, L. PERU, P. BRUNET, V. SHARMA, S. ZALZAL and M. D. MCKEE, *ibid.* **40**(2) (1998) 324.
19. E. LEITÃO, M. A. BARBOSA and K. DE GROOT, *J. Mater. Sci. Mater. Med.* **9**(9) (1998) 543.
20. S. M. SZE, Physics of Semiconductor Devices 2nd edn. (John Wiley and Sons, 1981).
21. T. HANAWA, Y. KAMIURA, S. YAMAMOTO, T. KOHGO, A. AMEMIYA, H. UKAI, K. MURAKAMI and K. ASAOKA, *J. Biomed. Mater. Res.* **36**(1) (1997) 131.
22. T. HANAWA, *Microstruct. Process.* **267**(2) (1999) 260.
23. E. WIESER, I. TSYGANOV, W. MATZ, H. REUTHER, S. OSWALD, T. PHAM and E. RICHTER, *Surf. Coat. Technol.* **111**(1) (1999) 103.
24. C. R. HOWLETT, *J. Biomed. Mater. Res.* **44**(3) (1999) 352.
25. Y. SUZUKI, M. KUSAKABE, M. KAIBARA, M. IWAKI, H. SASABE and T. NISHISAKA, *Nucl. Instr. Meth. Phys. Res.* **B91** (1994) 588.
26. J. CLOVER and M. GOWEN, *Bone* **15**(6) (1994) 585.
27. T. HANAWA, H. UKAI and K. MURAKAMI, *J. Electron. Spectrosc. Relat. Phenom.* **63**(4) (1993) 347.
28. C. D. WAGNER, L. E. DAVIS, ZELLER, J. A. TAYLOR, R. M. RAYMOND and L. H. GALE, *Surf. Interf. Anal.* **3**(5) (1981) 211.
29. SRIM 2000 J. F. Ziegler IBM-Research NY, USA
30. Profile Code Implant Sciences Co. Mass, USA
31. J. LAUSMAA, *J. Electron Spectrosc. Relat. Phenom.* **81**(3) (1996) 343.
32. E. MCCAFFERTY, J. P. WIGHTMAN and T. F. CROMER, *J. Electrochem. Soc.* **146**(8) (1999) 2849.
33. L. Q. WANG, A. N. SHULTZ, D. R. BAER and M. H. ENGELHARD, *J. Vac Sci. Technol. A* **14**(3) (1996) 1532.
34. T. HANAWA, *Mat. Sci. Eng.* **A267** (1999) 260.
35. M. T. PHAM, W. MATZ, H. REUTHER, E. RICHTER, G. STEINER and S. OSWALD, *Surf. Coat. Technol.* **128** (2000) 313.
36. M. T. PHAM, M. F. MAITZ, W. MATZ, H. REUTHER, E. RICHTER and G. STEINER, *Thin Solid Films.* **379**(1–2) (2000) 50.
37. J. E. ELLINGSEN, *Biomaterials* **12**(6) (1991) 593.

Received 10 July 2002
and accepted 8 April 2003